Precision Engineering 66 (2020) 125–134

Contents lists available at ScienceDirect

Precision Engineering

journal homepage: http://www.elsevier.com/locate/precision

Dynamic stiffness modification by internal features in additive manufacturing☆

Emma D. Betters [a,b,c,*], Justin West [b,c], Mark Noakes [c], Andrzej Nycz [c], Scott Smith [c], Tony L. Schmitz [b,c]

[a] Department of Mechanical Engineering and Engineering Science, University of North Carolina at Charlotte, 9201 University City Blvd, Charlotte, 28223, NC, USA
[b] Department of Mechanical, Aerospace, and Biomedical Engineering, University of Tennessee, Knoxville, 1512 Middle Dr, Knoxville, 37916, TN, USA
[c] Energy and Transportation Sciences Division, Oak Ridge National Laboratory, 2350 Cherahala Blvd NTRC-3, Knoxville, 37932, TN, USA

ARTICLE INFO

Keywords:
Additive manufacturing
Machining
Hybrid manufacturing
Structural dynamics
Dynamic stiffness

ABSTRACT

Dynamic stiffness, or the product of the modal stiffness and damping ratio, is an important consideration for the design of additively manufactured parts that will experience dynamic loading. This paper describes a demonstration component which was designed and manufactured in two configurations using a metal wire arc additive process. The first configuration was an open channel structure, while the second contained a dynamic absorber in the internal cavity. Frequency response measurements of the two components showed a significant magnitude reduction for the modified component at the original open channel structure's natural frequency and an overall increase in dynamic stiffness. Polymer damping material was then added to further increase the dynamic stiffness.

1. Introduction

In machining processes, the machine structure, spindle, holder, tool, and workpiece collectively compose a dynamic system that defines permissible cutting parameters [1]. Exceeding the limiting depth of cut for a particular spindle speeds leads to chatter, a self-excited vibration that produces large forces, poor surface finish, and may damage the workpiece, tool, or spindle. Practically, the dynamic stiffness of the machine tool determines the maximum chip width that can be prescribed without inducing chatter. In an effort to improve dynamic stiffness, or the product of the modal stiffness and damping ratio, the individual machine components can be designed specifically for higher stiffness and damping. One attractive target for improvement is the machine base. However, traditional casting processes for machine bases are geometrically limited, labor intensive, and expensive, so modifications to increase dynamic stiffness have been challenging to implement. It has been shown through simulation that dynamic absorbers can be optimally tuned and placed within the structure behind the spindle to improve machining performance [2]. Both passive and active systems have been implemented to alter the dynamics of fixturing and cantilevered tools and machine structures during machining operations [3,4].

An alternative approach is to use a wire arc additive manufacturing process to produce the machine base, thus eliminating the need for large castings. The additive approach offers significant design freedom for internal features which can be used to alter the dynamic characteristics of the system or to maximize the dynamic stiffness at a given frequency.

As a proof of concept, a pair of components was designed and fabricated to demonstrate the ability of the Metal Big Area Additive Manufacturing (mBAAM) process to print internal features intended to improve the structural dynamics (e.g., by altering the natural frequency or increasing the dynamics stiffness). The first component was an open channel attached to a base. The second component was identical, except for the addition of a dynamic absorber inside the open cavity. The absorber was designed to maximize the dynamic stiffness at the natural frequency of the original, open channel design. Fig. 1 shows the parameterized component geometries; Table 1 lists the dimensions. This

* Corresponding author. Energy and Transportation Sciences Division, Oak Ridge National Laboratory, 2350 Cherahala Blvd NTRC-3, Knoxville, TN, 37932, USA.
E-mail address: ebetters@vols.utk.edu (E.D. Betters).

https://doi.org/10.1016/j.precisioneng.2020.04.024
Received 28 January 2020; Received in revised form 25 March 2020; Accepted 14 April 2020
Available online 30 July 2020

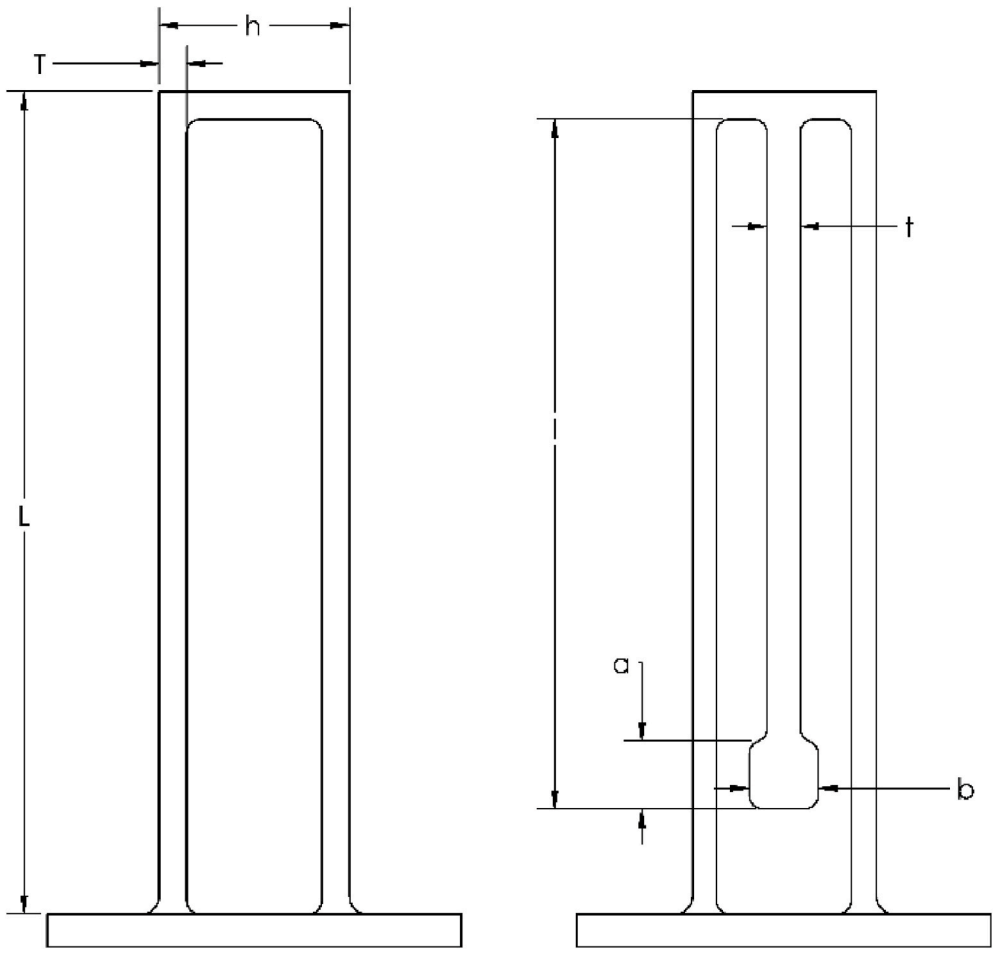

Fig. 1. Design dimensions for the (left) open channel and (right) open channel with dynamic absorber (w is the dimension into the page).

Table 1
Initial design dimensions (mm).

L	300
T	10
h	69
w	50
l	225
t	12
a	25
b	25

Table 2
Comparison of predicted and measured first natural frequencies (Hz).

Component	Predicted	Measured	% difference	Damping ratio (%)
No absorber	137.4	127.8	7.0	1.5
Absorber (unfilled) (f_{n1})	83.0	80.1	3.5	1.9
Absorber (unfilled) (f_{n2})	180.4	167.5	7.2	1.0
No absorber (filled)	–	124.0	–	2.3
Absorber (filled)	–	148.0	–	7.0

paper describes the design and finite element analysis validation of the dynamic absorber; the additive and subtractive manufacturing processes; and the measured frequency response functions (FRFs) for the final components (see Table 2).

2. Design and modeling

The dimensions of the open channel were designed with the limitations of the wire arc additive process in mind. The printed wall thickness was 12 mm (two weld beads) wide, which enabled the outer surfaces to be finish machined after printing. This is typical for components produced by mBAAM. The final machined dimensions (rather than rough printed dimensions) are shown in Table 1. The first natural frequency of the cantilever open channel was determined using finite element analysis (FEA). This frequency was used to design the dynamic absorber. FEA was completed using frequency analysis in SOLIDWORKS, where a fixed boundary condition was set for the base as shown in Fig. 2. A direct sparse solver was implemented and a standard 5 mm mesh with a 0.25 mm tolerance was used. The material properties required for the frequency solver are elastic modulus, density, and Poisson's ratio (210 GPa, 7800 kg/m^3, and 0.28 for steel). At the time of the design, it was uncertain which steel alloy would be used for printing, so general values were used. The natural frequency of the first bending mode was predicted to be 137.4 Hz for the open channel.

For the dynamic absorber design, the open channel was modeled as a single degree of freedom (SDOF) spring-mass system with an associated natural frequency $\omega_{n1} = \sqrt{\frac{k_1}{m_1}}$, where k_1 is the stiffness and m_1 is the mass. Similarly, the dynamic absorber element was modeled as a SDOF spring-mass system. The composite structure was therefore modeled by two spring-mass systems connected in series; see Fig. 3 [5].

For a harmonic force input, f_1, applied to the free end of the open channel model, the intent was to minimize the associated displacement, x_1, for a forcing frequency, ω_f, equal to the original structure's natural

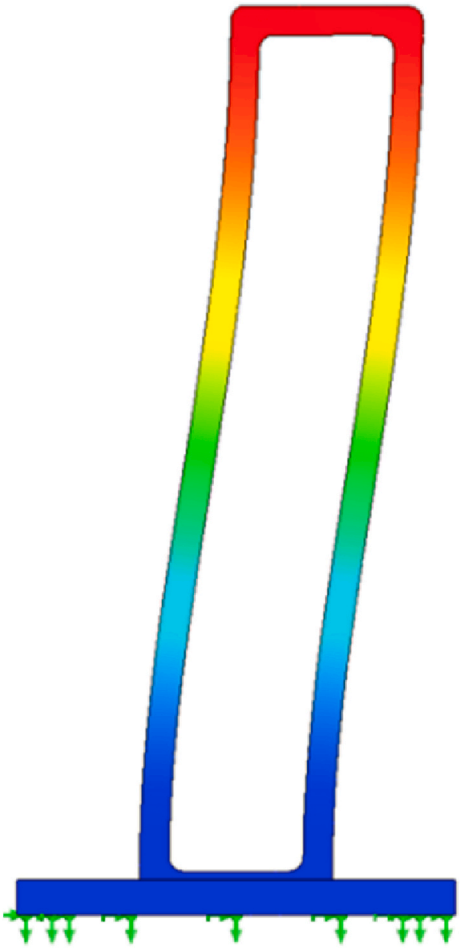

Fig. 2. The first FEA bending mode for the open channel is shown (137 Hz natural frequency).

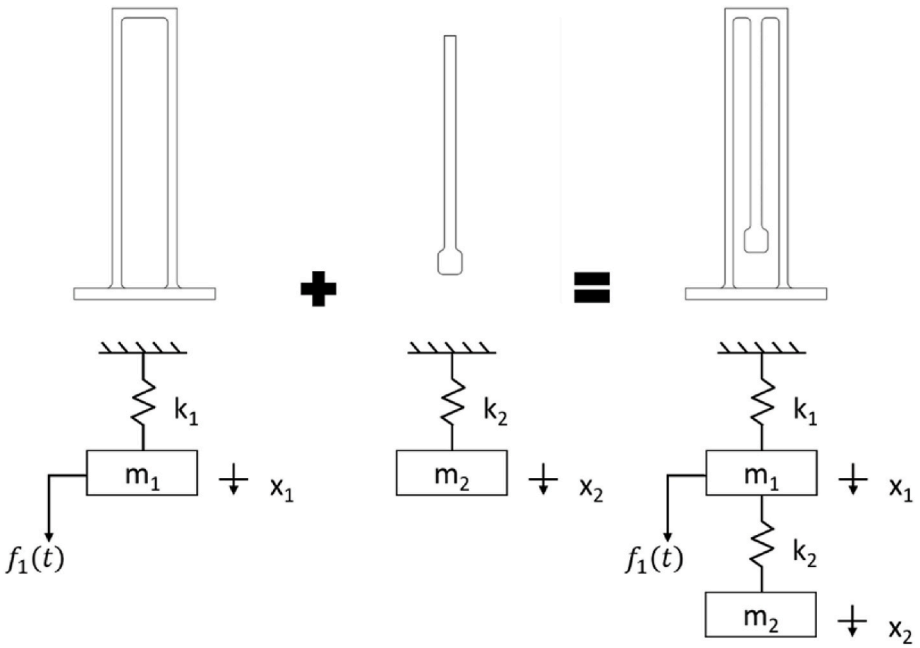

Fig. 3. The open channel and the dynamic absorber were modeled as SDOF systems. The channel-absorber has a 2DOF dynamic response.

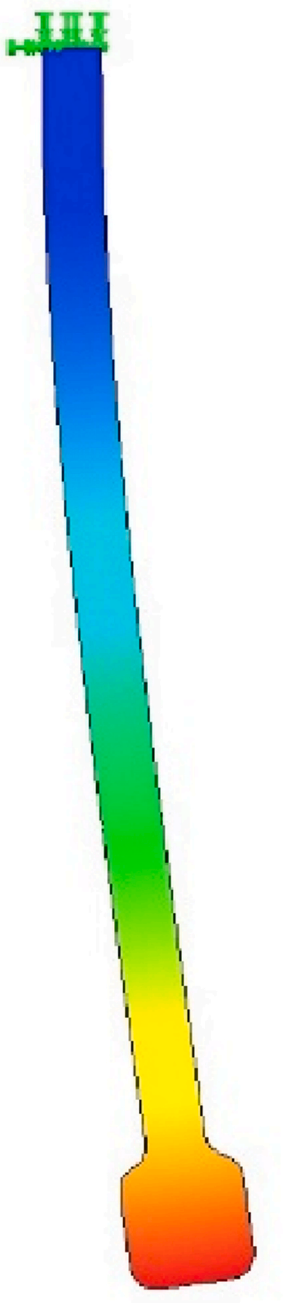

Fig. 4. The dynamic absorber was designed with a first bending natural frequency equal to the original open channel's natural frequency.

Fig. 5. (Left) External protective walls for the mBAAM system. (Right) The deposition head located above the printing position.

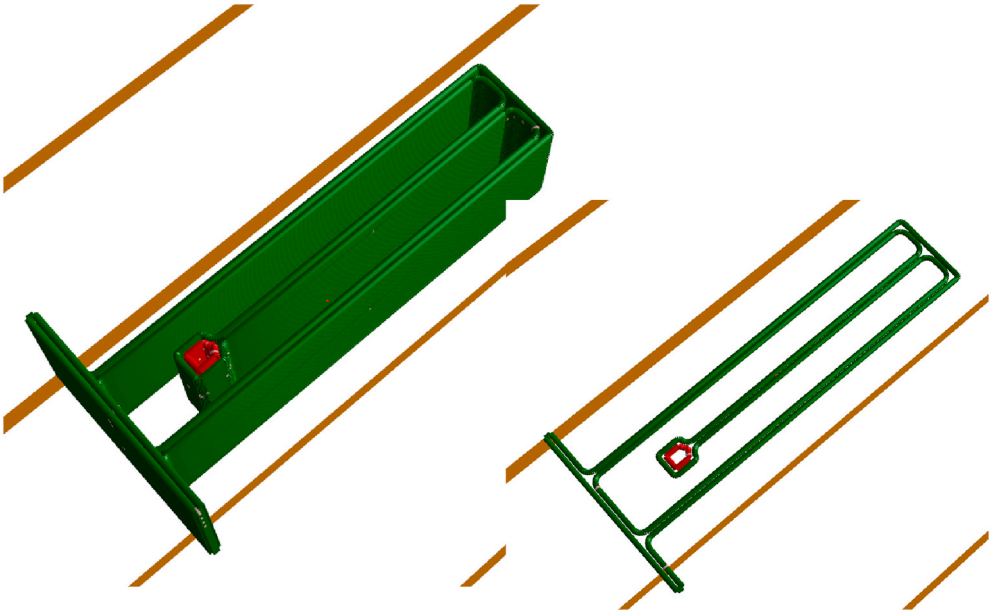

Fig. 6. The print path for the channel-absorber was created using the ORNL Slicer. (Left) The entire part is displayed. (Right) A single layer is shown.

frequency, ω_{n1}. The parameters for the dynamic absorber were selected so that the natural frequency of the absorber alone was equal to the first natural frequency of the open channel alone, $\omega_{n2} = \omega_{n1}$. This yields a new 2DOF system with two natural frequencies, one above and one below the original natural frequency. The spacing of the new frequencies is controlled by the size of the dynamic absorber mass (a small mass provides a small separation, while a mass close to the modal mass of the original system causes a larger separation).

The absorber was modeled with a fixed-free boundary condition as shown in Fig. 4, where its length (i.e., the dimension l shown in Fig. 1) was varied in FEA to obtain the desired natural frequency. The final values for the dynamic absorber are listed in Table 1.

3. Manufacturing

The hybrid manufacturing for the demonstration components was a joint effort between Oak Ridge National Laboratory (ORNL), where the additive process was completed, and the University of North Carolina at Charlotte, where machining was completed on the near net shape parts. The internal features of each component were left as-printed to demonstrate a broader application of this approach to systems where they cannot be accessed for further processing.

3.1. Additive

As noted, mBAAM is a wire arc-based process that uses gas metal arc welding (GMAW) with a robotic arm to carry the deposition torch [6–10]. The system is comprised of: IRB 2600 ABB manipulator, ABB IRC5 controller, PowerWave R500 Lincoln Electric welder, ABB IRBP-A750 positioner, safety system, desktop host workstation, shielding gas delivery system, and ventilation. The main components are enclosed by a protective wall that shields the operator from harmful UV radiation, heat, mechanical injury, and welding fumes as shown in Fig. 5.

As in most AM processes, mBAAM creates parts in a layer-by-layer fashion. Each layer consists of sets of sequenced weld beads. The

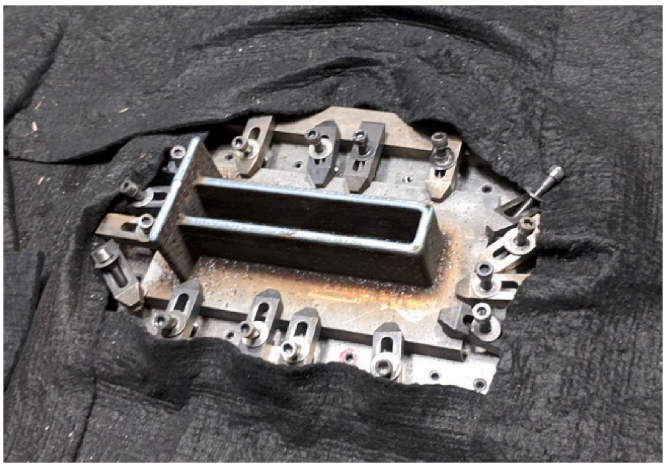

Fig. 7. The as-printed open channel (no absorber) is shown while still located on the deposition bed.

Fig. 9. The parts were clamped in a vise and a machining parallel was used as an indicating surface for the dial indicator to align the part.

Fig. 8. To machine the first side, the build plate was clamped to the machine table. The top surface was then faced.

sequence, among many variables, is dictated by the cross-sectional shape, function, and type of material. The same constraints apply to bead length, width, and overlap. The printed part is designed to be slightly oversized to enable machining that creates the desired surface finish and geometric accuracy.

The toolpath for printing is created by a process known as slicing. The part was built with a two-bead thick structure as shown in Fig. 6. The vertical print orientation of the part was chosen along the width of the part in order to avoid overhangs. This approach also minimized printing time since a single layer consisted of only two beads. The part toolpath was generated using the ORNL Slicer, a software suite used for both metal and polymer BAAM printers.

The printing process requires a base plate, a substrate with similar welding properties to the finished part. The substrate conducts the welding current and serves as a heat sink/transmitter. The substrate is typically mounted to the print bed using clamps. The bed and clamps are selected to provide sufficient stiffness to counteract the warping forces associated with the wire arc process. The bed also serves as the ultimate heat sink for the process.

Since the base plate can be mounted in any location or orientation on the deposition bed, a localization and orientation process is required. This is completed by directing the arm to three points which represent the origin and two axes of the new coordinate frame. Then, the system automatically recalculates the toolpath to match the part position and orientation with the base plate. The material (wire) used for manufacturing was Lincoln wire L59 (AWS ER70-S6) [11]. As noted, two parts were printed using this methodology: one with the dynamic absorber and one without. Fig. 7 displays the as-printed open channel with no absorber.

3.2. Subtractive

After the components were additively manufactured, all features were measured and compared to the nominal dimensions. The FEA model was updated using actual dimensions for the dynamic absorber. Due to the surface variation of the wire arc additive process, an average of measurements at 10 locations along each feature was applied. The updated model was used to determine the amount of material to be removed from each face. The predicted natural frequency of the finish machined open channel was 137.4 Hz.

The primary machining challenge was the lack of a clear datum. In the first operation, the build plate was assumed to be flat. It was stoned to remove debris from the build process and was clamped directly to the machine table. Each part was then faced to provide a reference once the build plate was removed; see Fig. 8. Next, the base plate was machined away and the associated surface machined to produce two parallel surfaces which could then be used for fixturing during the machining of the remaining sides. Prior to machining, the walls were sanded and stoned to remove debris and protrusions from the wire arc process. The previously machined front and back surfaces were clamped in a vise and a digital dial indicator was used to align the part; see Fig. 9. Each remaining surface was indicated and finished in the same way (see Fig. 10).

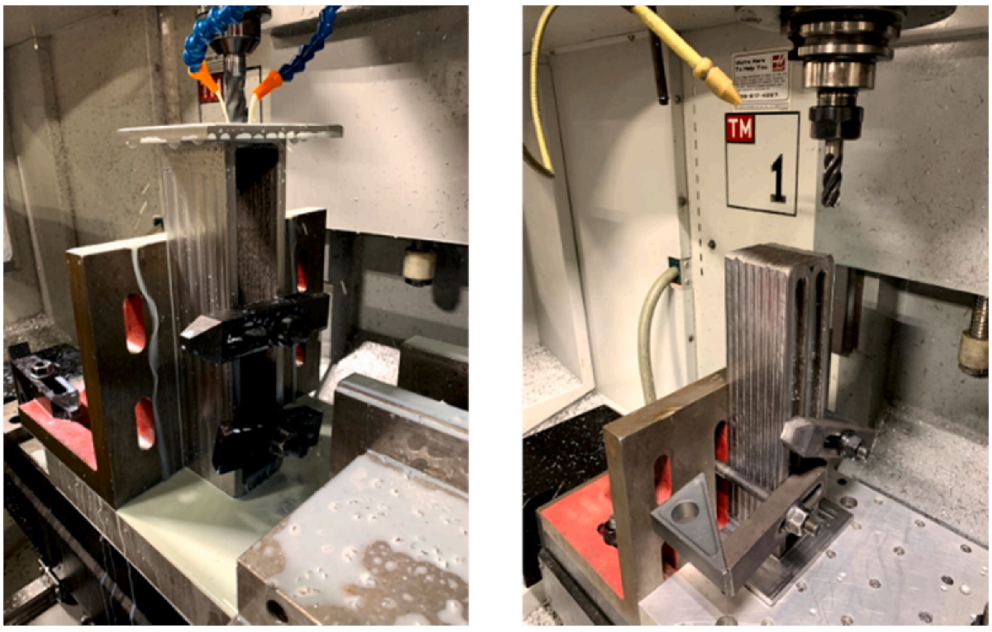

Fig. 10. The parts were fixtured to an angle plate to finish the top and bottom surfaces.

Fig. 11. Impact testing was used to measure the final part FRFs. For the FRF measurements, the parts were clamped to a rigid table to approximate fixed-free boundary conditions. A low-mass accelerometer is shown attached to the top right of the part.

The finished parts were clamped to a rigid table and a direct FRF was measured for both the open channel and the channel with the internal dynamic absorber. An instrumented hammer was used to excite the structure and a low mass accelerometer was used to record the vibration response for the FRF measurement; see Fig. 11.

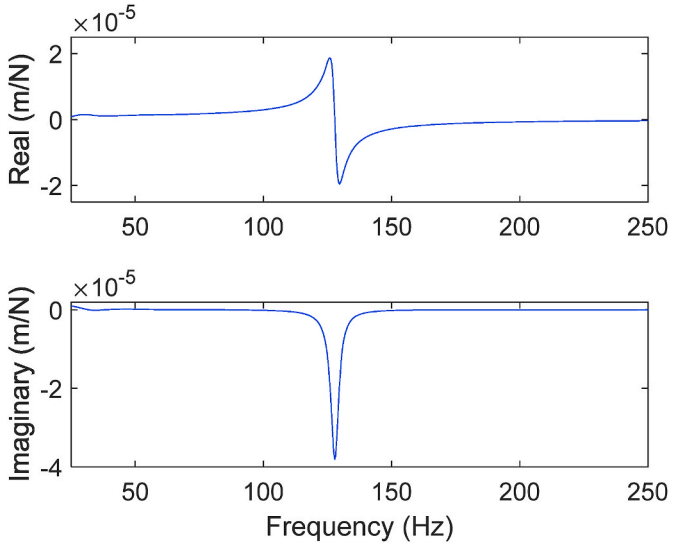

Fig. 12. The real (top) and imaginary (bottom) parts of the measured FRF for the open channel.

4. Results

The measured FRF for the open channel is shown in Fig. 12, where it is seen that the first natural frequency is 127.8 Hz. The predicted first natural frequency was 137.4 Hz (see Table 2). This variation was attributed to the surface undulations on the interior of the channel due to the bead geometry. These surface variations were not included in the modeling efforts and the additional material results in added mass and stiffness in the model versus the produced components.

The measured FRF for the channel with the dynamic absorber is displayed in Fig. 13, where the first and second natural frequencies are

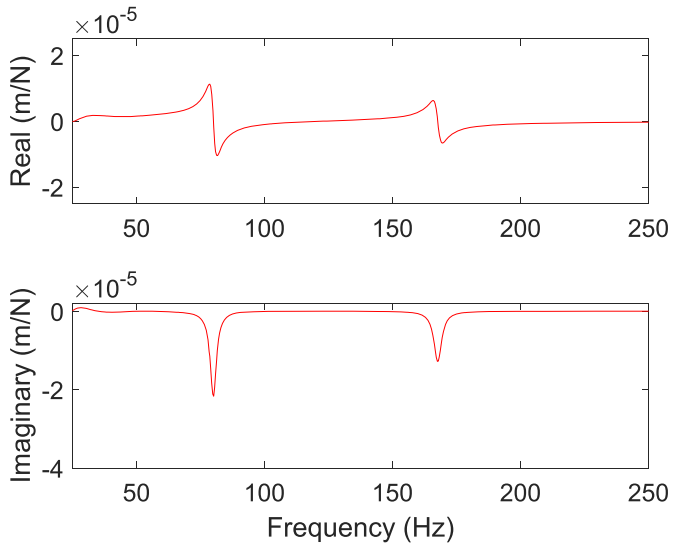

Fig. 13. The real (top) and imaginary (bottom) parts of the measured FRF for the channel with the dynamic absorber.

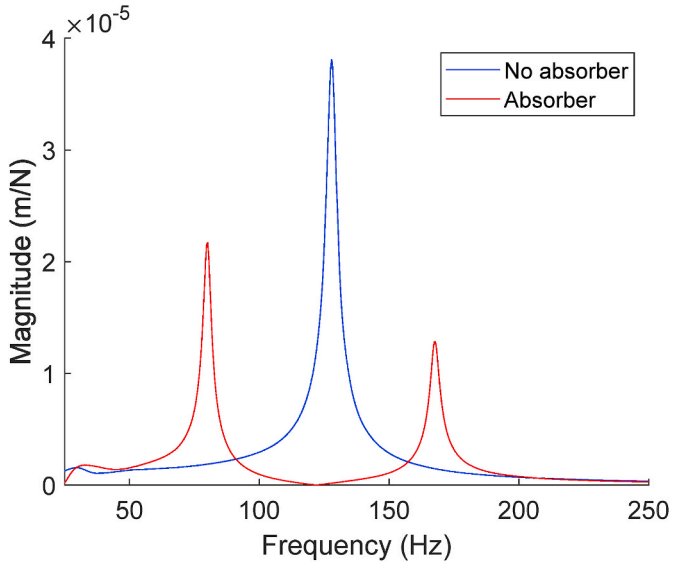

Fig. 14. Comparison of the measured FRF magnitudes for the two structures.

80.1 Hz and 167.5 Hz. The predicted values for these modes were 83.0 Hz and 180.4 Hz. Fig. 14 superimposes the magnitudes of the measured FRFs for both components, where it is observed that the response of the system with the dynamic absorber is minimized at the original natural frequency of the original open channel structure.

4.1. Added polymer damping

To provide additional damping, a polymer was poured into each of the cavities; see Fig. 15. The measured first natural frequency for the filled channel without the dynamic absorber was 124.0 Hz and with the dynamic absorber was 148.0 Hz. The respective viscous damping ratios of 0.02 and 0.07 were calculated from the measured FRF by peak picking, a method used to identify modal parameters from measured FRFs [5]. Fig. 16 shows the four results: open channel with no absorber; filled channel with no absorber; open channel with absorber; and filled channel with absorber. It is observed that the dynamic stiffness is dramatically increased by the polymer addition as shown by a decrease in the magnitudes.

5. Conclusions

Two wire arc additively manufactured components were produced to demonstrate design modifications that increase dynamic stiffness which can be expanded to much larger structures such as machine tool components. Here, an internal dynamic absorber was designed and incorporated as part of the printed part. It was shown that the system response with the added dynamic absorber was minimized at the natural frequency of the original open channel. Polymeric damping material was then added to further increase the dynamic stiffness. The disagreement between predicted and measured natural frequency is attributed to the undulations and inconsistent thickness of the additively produced walls which were not captured in the finite element model. In future work, a structured light scanner will be implemented in the initial metrology and modeling effort to more accurately capture variations in part geometry which may arise during the additive process. This will

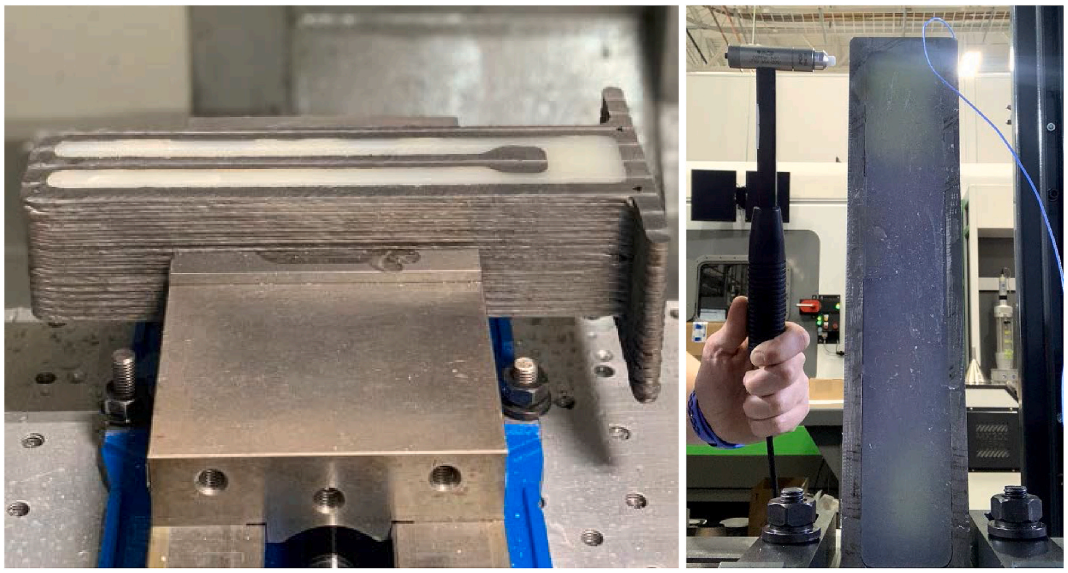

Fig. 15. Polymer was injected within the cavities to increase damping.

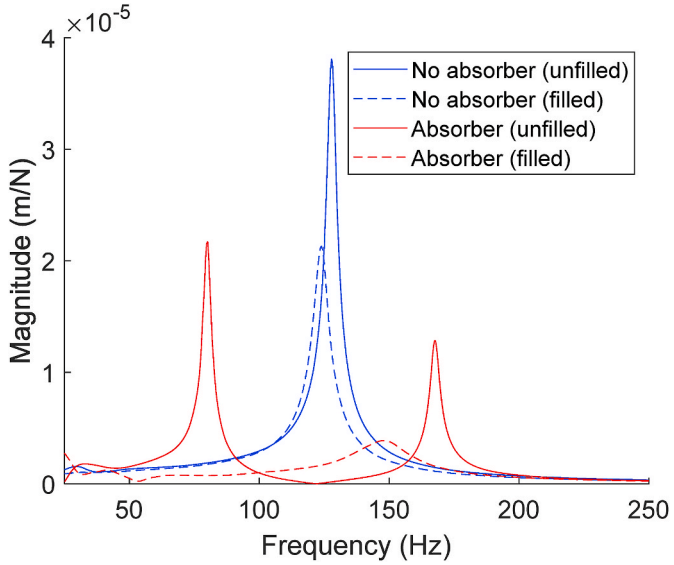

Fig. 16. Comparison of the FRF magnitudes for the three designs.

assist in providing a more accurate model for simulation. Additional components at larger scale may also be produced.

Declaration of competing interest

The authors declare that they have no known competing financial interests or personal relationships that could have appeared to influence the work reported in this paper.

Acknowledgements

This material is based upon work supported by the U.S. Department of Energy, Office of Science, Advanced Manufacturing Office under contract number DE-AC05-00OR22725, and used resources at the Manufacturing Demonstration Facility at Oak Ridge National Laboratory, a DOE Office of Science User Facility.

References

[1] Schmitz T, Smith KS. Machining dynamics: frequency response to improved productivity. second ed. New York, NY: Springer; 2019.
[2] Saadabad Navid Asmari, Moradi Hamed, Vossoughi Gholamreza. Global optimization and design of dynamic absorbers for chatter suppression in milling process with tool wear and process damping. Procedia CIRP 2014;21:360–6.
[3] Munoa Jokin, Iglesias Alex, Olarra Aitor, Dombovari Zoltan, Zatarain Mikel, Stepan Gabor. Design of self-tuneable mass damper for modular fixturing systems. CIRP Annals 2016;65(Issue 1):389–92.
[4] Rivin Eugene I, Kang Hongling. Enhancement of dynamic stability of cantilever tooling structures. Int J Mach Tool Manufact 1992;32(Issue 4):539–61.
[5] Schmitz T, Smith KS. Mechanical vibrations: modeling and measurement. New York, NY: Springer; 2012.
[6] Nycz A, Noakes M, Cader M. Additive manufacturing–A new challenge for automation and robotics. In: Conference on automation. Cham: Springer; 2018, March. p. 3–13.
[7] Shassere B, Nycz A, Noakes MW, Masuo C, Sridharan N. Correlation of microstructure and mechanical properties of metal Big Area additive manufacturing. Appl Sci 2019;9(4):787.
[8] Nycz A, Noakes MW, Richardson B, Messing A, Post B, Paul J, Flamm J, Love L. Challenges in making complex metal large-scale parts for additive manufacturing:

a case study based on the additive manufacturing excavator. In: Proceedings of the 28th annual international solid freeform fabrication symposium—an additive manufacturing conference; 2017.
[9] Greer C, Nycz A, Noakes M, Richardson B, Post B, Kurfess T, Love L. Introduction to the design rules for metal Big Area additive manufacturing. Additive Manufacturing 2019;27:159–66.
[10] Nycz A, Adediran AI, Noakes MW, Love LJ. January. Large scale metal additive techniques review. In: Proceedings of the 27th annual international solid freeform fabrication symposium; 2016.
[11] Lincoln Electric. Superarc L-59. https://www.lincolnelectric.com/assets/global/Products/Consumable_MIGGMAWWires-SuperArc-SuperArcL-59/c4104.pdf.